

Development of a Method for Chemical–Mechanical Preparation of the Surface of CdZnTe Substrates for HgCdTe-Based Infrared Focal-Plane Arrays

D. PELENC,^{1,4} J. MERLIN,¹ A. ETCHEBERRY,² P. BALLET,¹ X. BAUDRY,¹
D. BRELLIER,¹ V. DESTEFANIS,³ A. FERRON,¹ P. FOUGÈRES,³
D. GIOTTA,¹ C. GRANGIER,¹ L. MOLLARD,¹ A. PEREZ,¹ F. ROCHETTE,¹
L. RUBALDO,³ C. VAUX,³ J. VIGNERON,² and J.-P. ZANATTA¹

1.—CEA - Leti, MINATEC Campus, 17 Rue des Martyrs, 38054 Grenoble Cedex 9, France.
2.—Institut Lavoisier UVSQ-CNRS UMR 8180, 45 avenue des Etats Unis, 78035 Versailles,
France. 3.—Sofradir, Z.I., BP 21, 38113 Veurey-Voroize, France. 4.—e-mail: denis.pelenc@cea.fr

This paper reports the first implementation in our laboratory of a chemical–mechanical polishing (CMP) process for CdZnTe (CZT) substrates prepared for growth of HgCdTe layers by liquid phase epitaxy and molecular beam epitaxy. The process enables significant reduction of the thickness of the damaged zone induced by the mechanical polishing that must be etched away before epitaxy. Resulting improvements in surface morphology, in terms of waviness and density of point defects, are reported. The chemical state of surfaces polished by CMP was characterized by x-ray photoelectron spectroscopy. The chemical state was highly homogeneous; comparison with a reference surface is reported. End use assessment of this surface processing was compared with that of reference substrates by preparation of focal-plane arrays in the medium-wavelength infrared spectral range, by using epitaxial layers grown on substrates polished by different methods. The electro-optical performance of the detectors, in terms of photovoltaic noise operability, are reported. The results reveal that the state of this CMP surface is at the level of the best commercial substrates.

Key words: CdHgTe, chemical–mechanical polishing, x-ray photoelectron spectroscopy, focal-plane array

INTRODUCTION

The surface preparation of CdZnTe (CZT) substrates has an important effect on the quality of epitaxial layers of HgCdTe grown on these substrates and, consequently, on the performance of detectors for infrared applications. Surface processing of CZT substrates is usually conducted by successive steps of mechanical polishing with hard abrasives, which result in an imperfect, finely scratched surface, despite roughness in the super-polish range, i.e. < 1 nm root-mean square (RMS). In addition to these fine scratches, a sub-surface damaged zone with a depth

of several microns precludes direct epitaxy without further treatment. This damaged zone is usually removed by deep chemical etching which, in turn, has disadvantages, for example use of highly corrosive chemicals (e.g. bromine–methanol solutions) and alteration of the shape of the substrate surface, including roll-off and surface waviness. Deep chemical etching can also lead to point defects on the final surface, as the result of local variations in etch rate caused by material inhomogeneities encountered by the etch front.

For these reasons, there is a need for a surface treatment process which, by limiting the thickness of the sub-surface zone damaged during polishing, does not require such deep chemical etching before epitaxy. This objective can be met by addition of

(Received November 30, 2013; accepted April 8, 2014;
published online May 10, 2014)

chemical action to mechanical polishing, and was the reason for the development of chemical–mechanical polishing (CMP) of CdTe,^{1–3} inspired by processing of silicon wafers. Alternative methods have also been investigated, for example pure chemical polishing using a variety of bromine solutions,^{4,5} at the expense of the complexity of handling of such highly corrosive chemicals in large-scale production. These studies have focused mainly on the roughness³ and depth of sub-surface damage^{1,2} resulting from CMP, and on etch rate.^{4,5} The effects of CMP on the final performance of infrared focal-plane arrays (IRFPA) fabricated from epitaxial layers grown on CMP substrates have not yet been evaluated.

In this paper we report recent developments by the “French Atomic Energy and Alternative Energies Commission” (CEA) at the “Electronics and Information Technology Laboratory” (LETI) on the application of CMP to CZT substrates, comparative characterization of these surfaces and mechanically polished surfaces, and assessment of the state of their chemical surfaces by x-ray photoelectron spectroscopy (XPS). Finally, the final surface was evaluated for preparation of focal-plane arrays (FPA) in the middle wavelength infrared (MWIR) range, and shown to be suitable.

SURFACE PROCESSING OF CZT SUBSTRATES

We inserted two process steps after classical mechanical polishing of the CZT substrates—CMP surface processing and a series of post-polishing treatments. These two steps are described below.

Chemical–Mechanical Polishing

In this work, the emphasis was on final surface quality, so no particular attempt was made to optimize substrate flatness. The substrates were, therefore, simply waxed on to a holder adapted to the arm of a standard CMP machine and chemomechanically polished on a soft polyurethane pad attached to the machine plate rotating at 40 rpm.

In CMP, the chemical and mechanical action of the polishing results from use of a mixed polishing slurry containing an oxidizing chemical agent, which creates an oxide layer on the surface of the CZT, and an abrasive material consisting of spherical hard grains able to remove this oxide layer selectively. The diameter of these grains ranged from 10 to 100 nm. This mechanism has been already described for CMP of CdTe³ or, more generally, for compound semiconductors,⁶ and is widely applied in the semiconductor industry.⁷

In our case, special attention was devoted to the choice of these two components, to ensure good stability of the mixture, with no lump formation during the polishing.

Removal thickness was evaluated by use of a digital micrometer after, typically, polishing for 2 h,

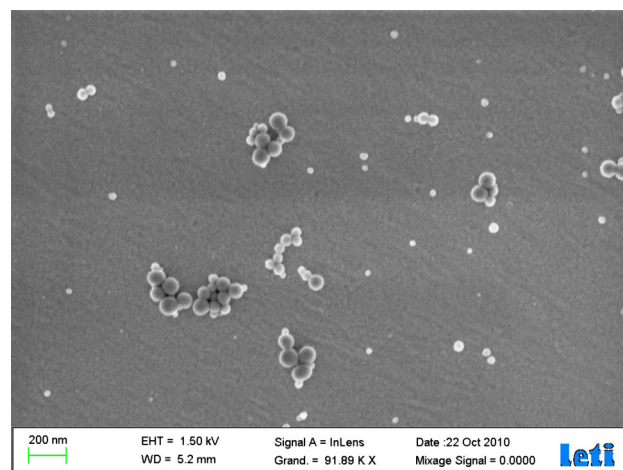


Fig. 1. SEM picture of the surface of a CZT substrate after CMP.

and cross-checked with weight-loss measurements. Rates of removal achieved under our CMP conditions were in the range 10–100 nm per minute, which was suitable for our application and is of the same order as obtained during wafer processing of silicon.⁸

Post-polishing Process

As illustrated by the scanning electron microscopy (SEM) picture in Fig. 1, taken after simple rinsing of the slurry from the surface by use of deionized water, residual abrasive grains can remain agglomerated on the surface. Removal of the polishing slurry after the CMP was, therefore, a major issue.

To address this problem, we developed a post-polishing process, which included several steps of cleaning and scrubbing with solvents and chemicals, which could be implemented without significantly degrading the roughness of the very delicate CZT surface.

Complete removal of the slurry was monitored by XPS. XPS spectra of the surface at the current stage of development and that obtained after simple rinsing with deionized water are compared in Fig. 2. Peaks arising from remaining abrasive slurry are clearly visible.

As will be apparent from the next section, it was still necessary to add to the post-polishing process slight chemical etching to remove a thin residual sub-surface damaged zone. The thickness of the zone removed by this weak etching was approximately one tenth that which needed to be removed after conventional mechanical polishing.

MORPHOLOGICAL CHARACTERIZATION

Final Surface Aspect and Roughness

As is apparent from the atomic force microscope (AFM) picture in Fig. 3a, fine scratch-shaped irregularities are still present on the CZT substrate

surface; slight etching of the surface was therefore required before epitaxy. Figure 3b shows the smoother surface obtained after this etching. Surface roughness, after CMP, the post-polishing process, and slight etching, as measured by AFM operated in tapping mode over a $1\text{ }\mu\text{m} \times 1\text{ }\mu\text{m}$ field, are given in Table I.

Advantages of CMP Over Conventional Mechanical Polishing

As mentioned in the Introduction, one advantage of CMP over mechanical polishing is the softer removal ensured by CMP, and the resulting smaller density of fine scratches after polishing. This advantage is apparent from Fig. 4, which compares the morphology of surfaces polished by the two methods, as observed by use of an optical interferometric micro-

scope. Although the roughness of the two surfaces is similar, the higher density of fine scratches resulting from mechanical polishing is clearly evident.

The advantages of reducing the chemically etched zone as a result of using the CMP process are illustrated in Figs. 5 and 6. Figure 5 is a comparison of substrate surface morphology, as observed by interferometric microscopy, after CMP, the post-polishing process, and slight etching of the surface (a) and after the deep chemical etching required after conventional mechanical polishing (b). Both pictures were taken strictly in the same zone of the substrate. The higher density of point defects induced by the deep chemical etching is obvious.

A similar comparison is made in Fig. 6, which shows interferograms obtained from the entire substrate surfaces after slight (a) and deep (b) chemical etching. The surface waviness induced by the deep chemical etching, mentioned in the Introduction, leads to irregular interference fringe curvature and small-scale variations in inter-fringe spacing (Fig. 6b). The peak-to-valley surface waviness amplitude, evaluated by use of an interferometric microscope, is approximately 20–30 nm, in agreement with typical $\lambda/10$ fringe deviations observed in Fig. 6b.

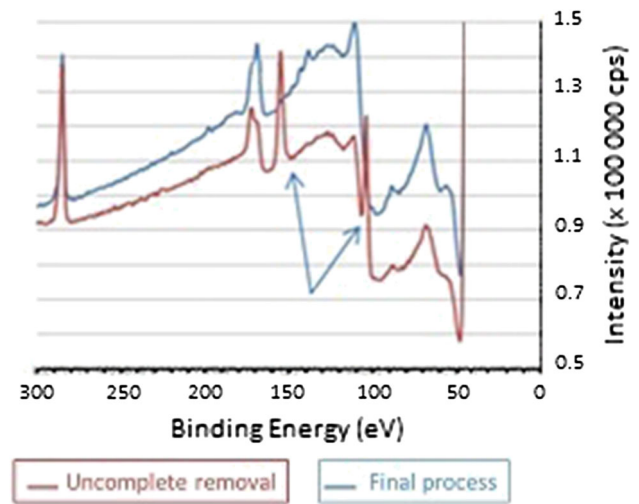


Fig. 2. XPS spectra of the surface before and after the implementation of post-polishing process (arrows indicate peaks arising from remaining abrasive grains).

Table I. Surface roughness after different processing steps.	
Surface processing step	RMS Roughness (nm), (field $1\text{ }\mu\text{m} \times 1\text{ }\mu\text{m}$, AFM in tapping mode)
After CMP	2.29
After post-polishing process	1.37
After slight etching	0.74

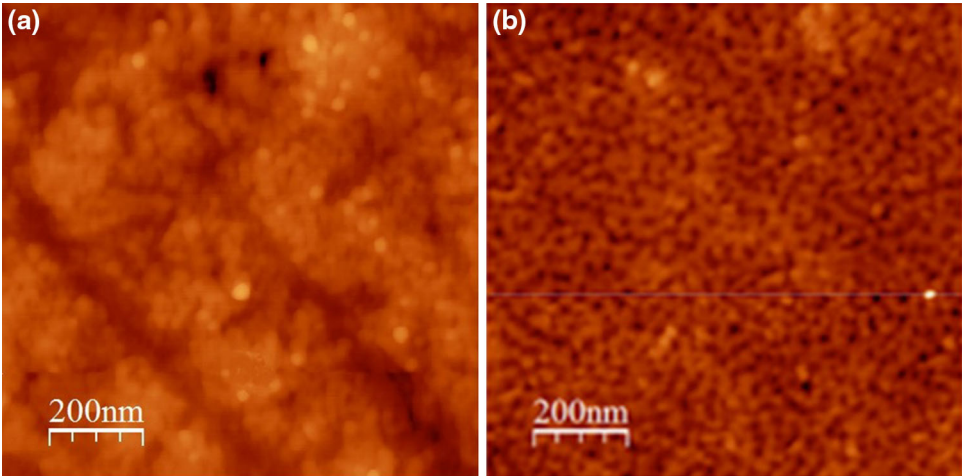


Fig. 3. AFM pictures of the CZT substrate surface after the post-polishing processes without any etching (a) and after slight chemical etching (b). The vertical grayscale is 10 nm in (a) and 4 nm in (b).

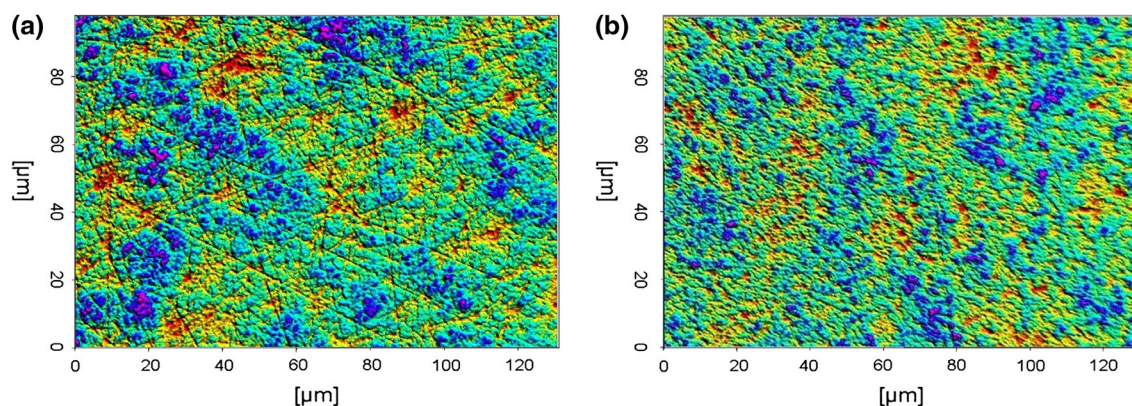


Fig. 4. Surface morphology of CZT substrates after fine mechanical polishing (roughness 0.87 nm RMS) (a) and CMP with post-polishing (roughness 0.59 nm RMS) (b). Objective $\times 40$. Field is $130\ \mu\text{m} \times 100\ \mu\text{m}$. The vertical color scale is 2.6 nm in (a) and 1.8 nm in (b).

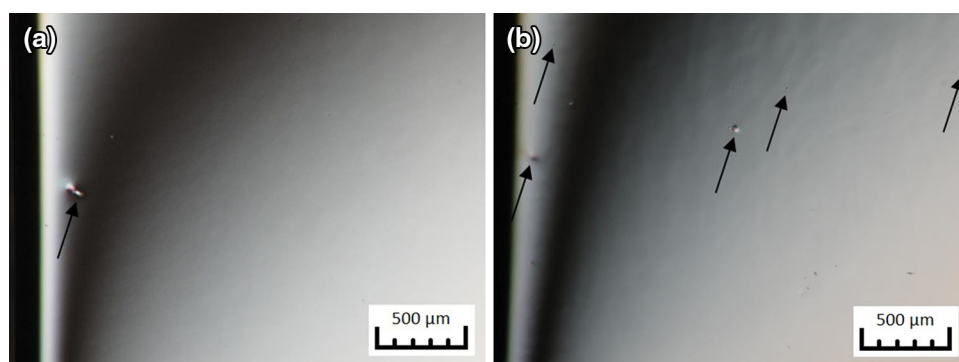


Fig. 5. Morphology of the surface of a CZT substrate after CMP followed by post-polishing surface treatment and slight chemical etching (a) and followed by deep chemical etching (b). Each arrow indicates a point defect. Field is $1.9\ \text{mm} \times 2.7\ \text{mm}$.

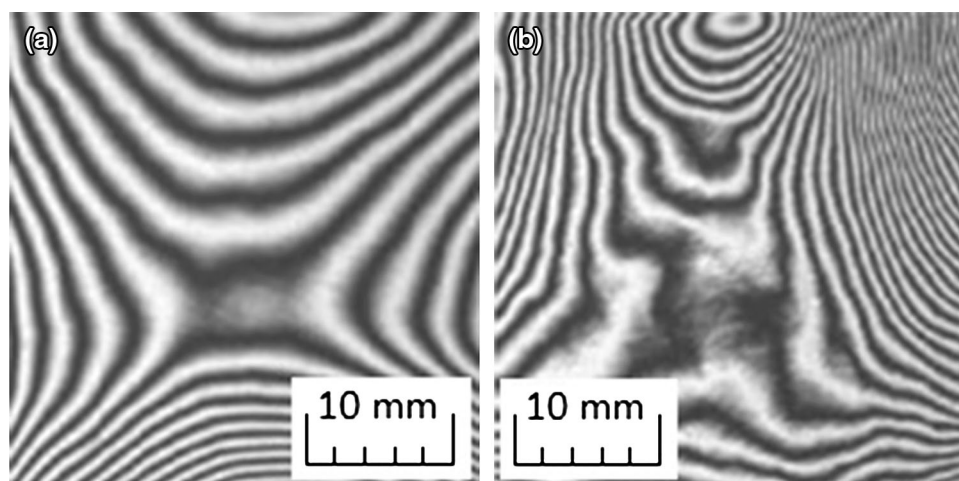


Fig. 6. Interferogram of a central area of a CZT substrate polished by CMP followed by post-polishing treatment and slight chemical etching (a) and followed by deep chemical etching (b). Field $35\ \text{mm} \times 35\ \text{mm}$. $\lambda = 633\ \text{nm}$.

XPS CHARACTERIZATION

The polished surfaces were characterized by XPS, which provides information about the chemical environment of the Te and Cd species located in the vicinity of the surface and is, therefore, well adapted to characterization of a polishing process.

Surface Uniformity

Uniformity of the chemical environment of Te and Cd throughout the surface of a $36 \times 38\ \text{mm}^2$ substrate polished by CMP was verified by comparison of spectra acquired at five points homogeneously distributed on the surface. Incident x-ray beam size

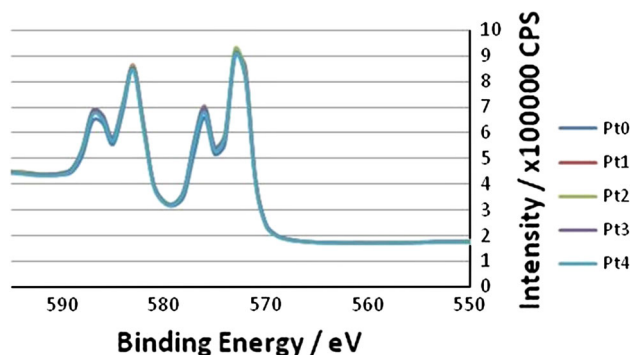


Fig. 7. XPS spectra of the 3d lines of Te at five locations over a CZT substrate after CMP.

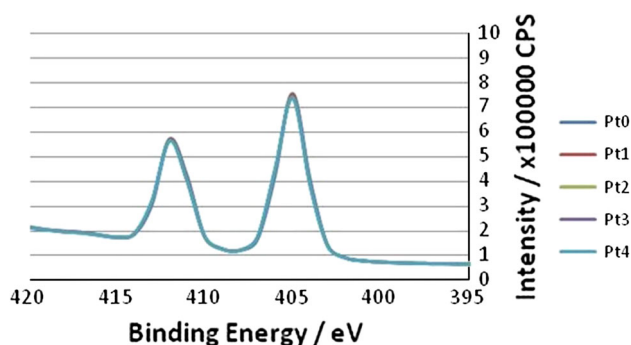


Fig. 8. XPS spectra of the 3d lines of Cd at five locations over a CZT substrate after CMP.

was approximately 1 mm, ensuring no overlap between the investigated zones. Figures 7 and 8 are plots of the 3d lines of tellurium and cadmium for these five points. The superposition of the lines clearly indicates excellent surface homogeneity of the chemical state of the substrate after CMP.

Tellurium Chemical Environment

The significant chemical displacement of the Te lines is indicative of chemical bonding of Te atoms located at the surface.⁹ This analysis was performed on substrates prepared by CMP and post-polishing treatments; the results were compared with those obtained from a commercial substrate regarded as the best on the market in terms of surface preparation.

Figures 9 and 10 show the 3d_{5/2} lines of Te obtained from a CMP substrate and from a reference substrate, respectively.

XPS line deconvolution leads to identification of three contributions to both spectra:

- the lowest Te_{CdZn} binding energy line at approximately 572.4 eV corresponding to Te bonded to Cd or Zn;
- the highest binding energy line at approximately 576 eV corresponding to Te oxides, shifted by 3.6 eV relative to Te_{CdZn} ; and

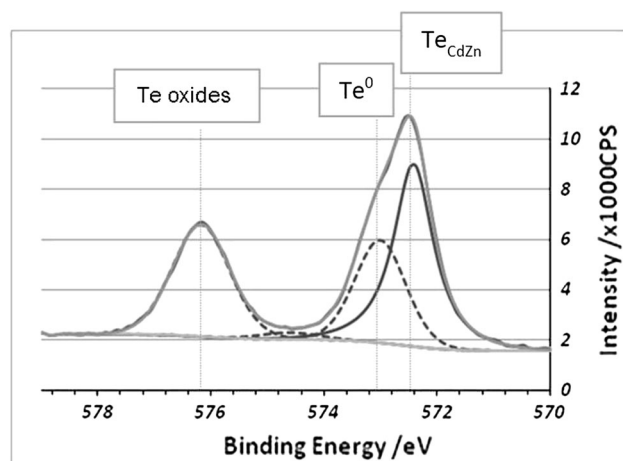


Fig. 9. XPS spectra of the 3d_{5/2} lines of Te from a CMP substrate.

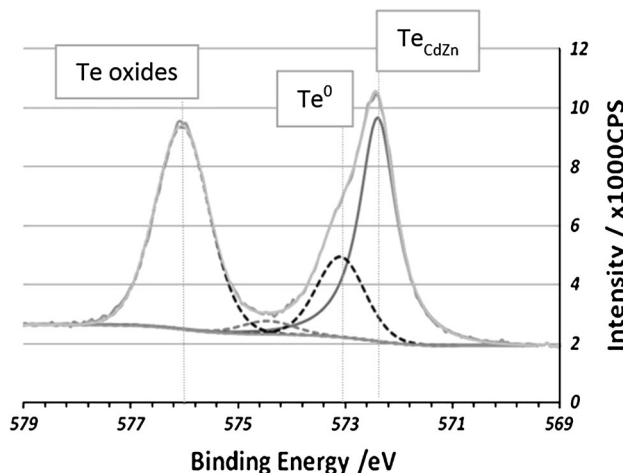


Fig. 10. XPS spectra of the 3d_{5/2} lines of Te from a reference substrate.

- an intermediate Te° line at approximately 573 eV corresponding to elemental Tellurium, shifted by 0.6 eV relative to Te_{CdZn} .

These shifts are in full agreement with previously reported studies⁹ of oxidized CZT surfaces.

The occurrence of the three peaks of the 3d_{5/2} lines of Te from both the CMP substrate and the reference commercial substrate is a clear indication that the chemical surface states of these surfaces are very similar; this is indicative of similar behavior during the epitaxial growth.

CMP VALIDATION BY MWIR FPA FABRICATION AND CHARACTERIZATION

The CMP surface processing was validated by comparative characterization of MWIR IRFPAs for which the same technological steps had been followed, in parallel, except for the method of polishing of the substrate, namely conventional polishing or the new CMP and post-polishing process. These

comparisons were performed for IRFPA prepared from HgCdTe layers grown either by liquid-phase epitaxy (LPE) or molecular-beam epitaxy (MBE), which are reported successively below.

MWIR FPA Based on LPE Layers

Two (111) oriented CZT substrates were used for this comparison. Substrate “M” was mechanically polished and deep chemical etching of the surface was conducted before LPE. The surface of substrate “CMP” was prepared by CMP followed by the post-polishing treatment mentioned in the previous section. Slight chemical etching was performed before HgCdTe epitaxy. The characteristics of the LPE layers are given in Table II

n on *p* LETI standard technology¹⁰ was performed with these layers for fabrication of MWIR FPAs. The FPA was a TV/4 format, 320×256 pixels, $30 \mu\text{m}$ pitch array. The operating temperature was 80 K, with a field of view (FOV) of 30° in front of a 298 K black body. Noise features measured for the FPA named “M” and “CMP”, prepared using epilayers grown on substrates M and CMP, respectively are summarized in Table III. The current noise of the photodiode is converted into output tension noise, as delivered by the read out integrated circuit. Operability is defined as the proportion of pixels with a noise value at $\pm 50\%$ of the average value.

The noise equivalent temperature difference (NETD) features of FPA “M” and “CMP” are summarized in Table IV. The NETD operability is defined as the number of pixels with an NETD within $\pm 100\%$ of the mean NETD. NETD histograms of both FPA are compared in Fig. 11.

The operability of each FPA is nearly equal, and both correspond to standard values achieved by use of this MWIR technology implemented for several years in this laboratory, and for which noise operability is known to be sensitive to material defects. Therefore, this first FPA test is a good sign of the absence of flaws which would have hampered this indicator.

MWIR FPA Based on MBE Layers

Because surface requirements for MBE are harder to meet than for LPE, this second comparison was more demanding. For this evaluation, two (211)-oriented CZT substrates—named CMP1 and CMP2 hereafter—were prepared by CMP and post-polishing

treatments as described above. As for the LPE substrates mentioned above, slight chemical etching was conducted before HgCdTe MBE epitaxy. A commercial substrate—named R hereafter—was used as reference. This commercial supply of CZT substrate is regarded as a reference in our laboratory, as the result of the high-quality MBE layers grown on these substrates.¹¹ The characteristics of the MBE layers are given in Table V.

The *n* on *p* LETI standard technology was performed with these layers for fabrication of MWIR FPAs. The FPA was a TV/4 format, 320×256 pixels, $30 \mu\text{m}$ pitch array. The operating temperature was 80 K, with an FOV of 30° in front of a 298 K black body.

Noise features measured for FPA named “CMP1”, “CMP2”, and R prepared using epilayers grown on the corresponding substrates are summarized in Table VI. More details on the sensitivity to material defects of the noise operability can be found elsewhere.¹²

These results match standard values for this technology. The operability of the FPA “CMP” is in the same range as that obtained on IRFPA processed in the same batch using the best commercial substrates, and is even higher for FPA “CMP1”.

Table III. Comparison of the noise features of the FPA based on LPE layers.

Noise features	FPA “M”	FPA “CMP”
Average value ($\mu\text{V RMS}$)	344	322
Dispersion (%)	12.2	13
Operability (%)	99.7	99.68
Number of defects (over 81920 pixels)	244	265

Table IV. Comparison of the NETD noise features of the FPA based on LPE layers.

NETD noise feature	FPA “M”	FPA “CMP”
Average value (mK)	9.83	9.80
Dispersion (%)	8.4	8.2
Operability (%)	99.78	99.80
Number of defects (over 81920 pixels)	182	165

Table II. Characteristics of the LPE layers used for the comparison of MWIR FPA performances.

	Substrate M	Substrate CMP
Surface processing method	Conventional (mechanical + deep chemical etching)	CMP + post-polishing treatment
Cut-off wavelength @ 300 K (μm)	4.49	4.56
Epilayer thickness (μm)	7.9	8.2

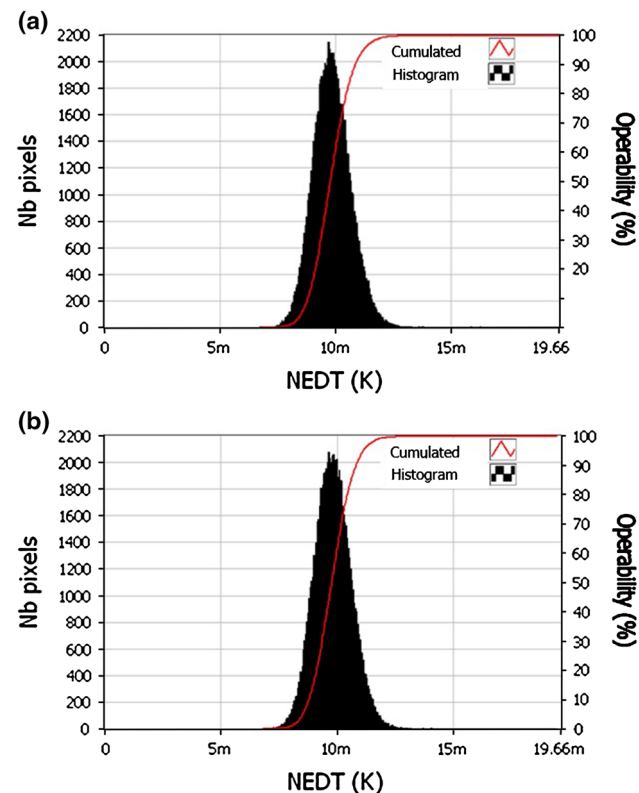


Fig. 11. NETD histograms of FPA “M” (a) and “CMP” (b).

Table V. Characteristics of the MBE layers used for the comparison of MWIR FPA performances.

	Substrate CMP1	Substrate CMP2	Substrate R
Cut-off wavelength @ 77 K (μm)	4.96	4.96	4.96
Epilayer thickness (μm)	7.6	7.6	7.8

Table VI. Comparison of the noise features of the FPA based on MBE layers.

Noise features	FPA “CMP1”	FPA “CMP2”	FPA “R”
Average value ($\mu\text{V RMS}$)	311	327	339
Dispersion (%)	13.4	13.3	12.4
Operability (%)	99.23	98.64	98.91

CONCLUSION

At LETI we have successfully implemented a new technique for surface processing of CZT substrates. The method includes CMP and post-polishing cleaning of the surface. This process enables reduction in the thickness that must be chemically etched away

before epitaxy. This reduction has been proved to lead to substrates with lower surface waviness and a lower density of point defects. Typical roughness resulting from this processing is 0.74 nm RMS.

The chemical state of the surface was characterized by XPS and found to be homogeneous over the whole surface. Comparison of the Te 3d5/2 peaks from a CMP substrate with those from a reference substrate revealed the high similarity of the two materials, with the characteristic peaks of Te oxides and elemental Tellurium.

HgCdTe layers were grown on these CMP-processed substrate surfaces, by both LPE and MBE, and used to fabricate FPAs in the MWIR range. Standard reference substrates were processed in parallel for comparison. The noise operability of FPA prepared with LPE layers was 99.78% and 99.80% for CMP substrate and standard substrate, respectively. For FPA prepared using MBE layers, noise operability was very similar, irrespective of the process used for preparation of the substrate.

In conclusion, although a larger statistical population must be used to confirm these results, the chemical mechanical process developed at LETI has been shown to furnish results similar to those from the best commercial substrates. After successful validation for the MWIR range, the next step will be to evaluate the CMP process for the more demanding LWIR spectral range.

Furthermore, this validation of the final state after polishing enables implementation of this method and improvement of results from previous mechanical polishing steps, for example surface flatness and parallelism.

ACKNOWLEDGEMENTS

The authors are grateful to the Délégation Générale de l’Armement of the French Ministry of Défense for its support in the development of this technology.

REFERENCES

1. D.F. Weirauch, *J. Electrochem. Soc.* 132, 250 (1985). doi: [10.1149/1.2113775](https://doi.org/10.1149/1.2113775).
2. A. Nourizi-Khorrasani, M.A. Lunn, I.P. Jones, and P.S. Dobson, *J. Cryst. Growth* 102, 1069 (1990).
3. P. Moravec, P. Hoschl, J. Franc, E. Belas, R. Fesh, R. Grill, P. Horodysky, and P. Praus, *J. Electron. Mater.* 35, 1206 (2006).
4. Z.F. Tomashik, I.I. Gnativ, V.N. Tomashik, and I.B. Stratiichuk, *Russ. J. Inorg. Chem.* 52, 1156 (2007).
5. Z.F. Tomashik, I.I. Hnativ, V.N. Tomashik, and I.B. Stratiychuk, *Russ. J. Inorg. Chem.* 51, 1320 (2006).
6. I.D. Marinescu, H.K. Tonshoff, and I. Inasaki, *Handbook of Ceramic Grinding and Polishing* (New York: Elsevier, 1999), p. 414.
7. Oliver, *Chemical-Mechanical Planarization of Semiconductor Materials* (Berlin: Springer, 2004), p. 215.
8. Y. Liu, K. Zhang, F. Wang, and W. Di, *Microelectron. Eng.* 66, 438 (2003).
9. G. Badano, A. Million, B. Canava, P. Tran-Van, and A. Etcheberry, *J. Electron. Mater.* 36, 1077 (2007).
10. G. Destéfani, *J. Cryst. Growth* 86, 770 (1988).

11. P. Ballet, F. Noël, F. Pottier, S. Plissard, J.P. Zanatta, J. Baylet, O. Gravrand, E. De Borniol, S. Martin, P. Castelein, J.P. Chamonal, A. Million, and G. Destéfanis, *J. Electron. Mater.* 33, 667 (2004).
12. O. Gravrand, G. Destéfanis, S. Bisotto, N. Baier, J. Rothman, L. Mollard, D. Brellier, L. Rubaldo, A. Kerlain, V. Destéfanis, and M. Vuillermet, *J. Electron. Mater.* 42, 3349 (2013).